JGR Space Physics

RESEARCH ARTICLE
10.1029/2023JA031285

Whether Sudden Stratospheric Warming Effects Are Seen in the Midlatitude Thermosphere of the Opposite Hemisphere?

Andrey V. Mikhailov[1,2] **and Loredana Perrone**[2]

[1]Pushkov Institute of Terrestrial Magnetism, Moscow, Russia, [2]Istituto Nazionale di Geofisica e Vulcanologia (INGV), Roma, Italia

Key Points:

- Arctic Sudden Stratospheric Warmings (SSWs) always result in a simultaneous foF2 depression observed at some stations in the Northern Hemisphere
- Pronounced thermospheric SSW effects in the opposite (Southern) Hemisphere may be expected only for strong major Arctic SSW events
- TEC increase in the western region of North America during the minor Antarctic SSW was not related to thermospheric parameters changes

Correspondence to:

L. Perrone,
loredana.perrone@ingv.it

Citation:

Mikhailov, A. V., & Perrone, L. (2023). Whether sudden stratospheric warming effects are seen in the midlatitude thermosphere of the opposite hemisphere? *Journal of Geophysical Research: Space Physics*, *128*, e2023JA031285. https://doi.org/10.1029/2023JA031285

Received 2 JAN 2023
Accepted 12 MAY 2023

Author Contributions:

Conceptualization: Andrey V. Mikhailov
Methodology: Andrey V. Mikhailov, Loredana Perrone
Software: Andrey V. Mikhailov, Loredana Perrone
Validation: Andrey V. Mikhailov, Loredana Perrone
Writing – original draft: Andrey V. Mikhailov, Loredana Perrone

Abstract The reaction of midlatitude daytime foF_2 and thermospheric parameters in two Hemispheres has been analyzed for a minor Arctic Sudden Stratospheric Warming (SSW) in January 2008, three major Arctic SSWs in January 2006, 2009, 2013, and a minor Antarctic SSW in September 2019. Arctic SSWs always result in a simultaneous foF_2 depression observed at some stations in the Northern Hemisphere but not necessary in the opposite Hemisphere, that is, not all SSWs have global appearance. Thermospheric parameters retrieved from ionospheric observations in two Hemispheres manifest a dependence on the type of SSW (major/minor) and its magnitude. Pronounced thermospheric SSW effects in the opposite (Southern) Hemisphere may be expected only for strong major Arctic SSW events. Retrieved exospheric temperature does not manifest any visible reaction to SSWs both for major and minor SSW events. The duration of foF_2 and atomic oxygen decrease related to SSW is 3–5 days in the vicinity of the SSW peak. Both observed neutral gas density and retrieved thermospheric parameters do not manifest a significant difference comparing western and eastern regions of North America during the minor Antarctic SSW in September 2019. Therefore, the previously reported (80–100%) increase in TEC in the western region of North America was not related with variations of neutral composition and winds.

1. Introduction

The reaction of thermosphere and ionosphere to Sudden Stratospheric Warming (SSW) is an excellent example of the impact from below on the Earth's upper atmosphere. This issue is widely discussed in the literature. A review of papers devoted to foF_2 effects at middle latitudes related to SSWs was done in our previous paper (Mikhailov et al., 2021), see also a comprehensive review by Goncharenko, Harvey, Liu, and Pedatella (2021). It should be stressed that among indirect methods only observations of electron concentration in the F-region may indicate the state of the surrounding thermosphere (neutral composition, temperature, winds) while total electron content (TEC) observations widely used in SSW considerations is not a proper parameter for thermospheric analyses. TEC includes the plasmaspheric part which is not related to the underlying F_2-region but reflects the state of high-latitude ionosphere. Therefore, we do not here review foF_2 and TEC observations during SSW events. The present paper is devoted to SSW thermospheric effects simultaneously observed in two Hemispheres during SSWs and we will consider previously obtained observational results only under this angle. Numerous model simulations are also omitted here as their correctness is always questionable (e.g., Pedatella et al., 2014).

Liu et al. (2011) analyzing CHAMP and GRACE neutral gas density (ρ) observations during the major SSW in January 2009 revealed a significant ρ decrease across both hemispheres with the minimum on 24 January for the afternoon (16–18) LT sector. Further, authors found that the Southern Hemisphere experienced a larger relative density decrease than the Northern one. The observed depression in neutral density as well as in electron concentration measured on board the CHAMP satellite in the equatorial ($\pm 30°$) region was attributed to the thermosphere cooling initiated by SSW.

Observations from the recently launched Global-Scale Observations of the Limb and Disk (GOLD) instrument on the geostationary SES-14 communications satellite reveal a substantial response of the mean state of the thermosphere to the major SSW event in late December 2018 to early January 2019 (Oberheide et al., 2020). The observed column O/N_2 ratio depletion of more than 10% started at the onset of the SSW, maximized at the time of the stratospheric wind reversal, and recovered toward the end of the SSW.

Yamazaki et al. (2015) investigated possible impact of SSWs on the thermosphere by using long-term data of the global average thermospheric total mass density derived from satellite orbital drag during 1967–2013. A

Table 1
List of Stations Used in the Analysis

Station	Geographic coordinates	Station	Geographic coordinates
Rome	41.9°N, 12.5°E	Hermanus	34.4°S, 19.2°E
Athens	38.0°N, 23.5°E	Grahamstown	33.3°S, 26.5°E
Roquetes	40.8°N, 0.5°E	Christchurch	43.6°S, 172.8°E
Millstone Hill	42.6°N, 288.5°E	Canberra	35.3°S, 149.0°E
Point Arguello	34.8°N, 239.5°E	Hobart	42.9°S, 147.3°E
Boulder	40.0°N, 254.7°E		

Note. (Reinisch & Galkin, 2011; Upper Atmosphere Physics, 2020)

superposed epoch analysis of 37 SSW events manifested a density reduction of 3–7% at 250–575 km with the relative density perturbation being greater at higher altitudes. The temperature perturbation is estimated to be −7.0 K at 400 km.

Goncharenko, Harvey, Greer, et al. (2021) have reported strong (up to 80−100%) positive anomalies in the daytime TEC and an increase of the thermospheric O/N_2 ratio in the western region of North America during the Antarctic SSW in September 2019. However, central and eastern parts of North America have manifested moderate suppression of TEC reaching 20–40% of the baseline. The authors suggest that changes in thermospheric zonal wind play a major role in the formation of ionospheric anomalies, especially over western North America. These results raise a number of questions (see Section 4).

The aims of the paper may be formulated as follows:

1. To analyze the reaction of ionospheric (foF_2) and thermospheric (neutral composition, temperature, winds) parameters at midlatitudes of both Hemispheres to the minor Arctic SSW in January 2008 and three major Arctic SSWs in January 2009, January 2013, and January 2006.
2. To consider ionospheric and thermospheric effects to the minor Antarctic September 2019 SSW at middle latitudes of the North America where Goncharenko, Harvey, Greer, et al. (2021) have observed a large TEC anomaly presumably related to this SSW.

2. Observations and the Method of Analysis

Routine ionosonde observations at midlatitude stations in the Northern and Southern Hemisphere (Table 1) were used for the periods of three major Arctic SSWs (in January 2009, January 2013, and January 2006) and the minor Arctic SSW in January 2008. A special analysis was devoted to the ionospheric and thermospheric effects at the midlatitudes of Northern America during the minor Antarctic SSW in September 2019.

Interpolated over 11–13 LT foF_2 observations (using 5–15 min data when available) were used to find noontime relative foF_2/foF_{2med} deviations for the periods in question. Observed monthly median foF_2 used as a background in our analysis were interpolated for each day of a month using three adjacent months. Keeping in mind that observed foF_2 monthly medians may bear the SSW effects, we have controlled them using medians from the global empirical model GDMF2 by Shubin and Deminov (2019).

Daytime midlatitude foF_2 is closely related to the state of surrounding thermosphere (neutral composition, temperature, winds). Our method (Perrone & Mikhailov, 2018) to retrieve thermospheric parameters from ionospheric observations was used in the analysis. The basic version of this method utilizes observed noontime f_oF_2 and plasma frequencies at 180 km height, f_{180} for (10, 11, 12, 13, 14) LT, both observations may be taken from SAO files (Reinisch et al., 2004) at the stations where DPS-4 are installed. This strongly confines the list of available stations in the Southern Hemisphere. During summer season when foF_1 is well-pronounced on vertical sounding ionograms the method allows us to use observed foF_1 instead of f_{180} and this possibility was used at Hobart not equipped with DPS-4. An extended version of our method additionally uses observed neutral gas density (ρ) as a fitted parameter. Neutral gas density observations with CHAMP/STAR, GOCE, and Swarm (March et al., 2021; Siemes et al., 2016; van den Ijssel et al., 2020) satellites were used in the analysis. Inclusion of neutral density into the retrieval process increases the reliability of the obtained results. In this case the inferred neutral composition ([O], $[N_2]$, $[O_2]$ concentrations), temperature T_{ex} along with vertical plasma drift W and total solar EUV ionizing flux are found consistently with the observed neutral gas density.

Daytime neutral densities observed in the vicinity of ionosonde station were reduced to 12 LT and the location of ionosonde using the MSISE00 thermospheric model (Picone et al., 2002). The height of observed ρ used in our analysis was taken directly from the orbit not to introduce additional inaccuracy related to possible imperfectness of T_{ex} in MSISE00. The retrieved neutral gas density $\rho = m_1[O] + m_2[O_2] + m_3[N_2]$ does not include the contribution of [He] and [N] therefore the observed ρ were corrected using MSISE00. This correction is small (1–2)% for CHAMP/STAR observations at heights of ∼330 km in 2008–2009 (for GOCE even less due to low satellite orbits) while it is of (5–6)% for Swarm data obtained at heights of ∼438 km in 2019.

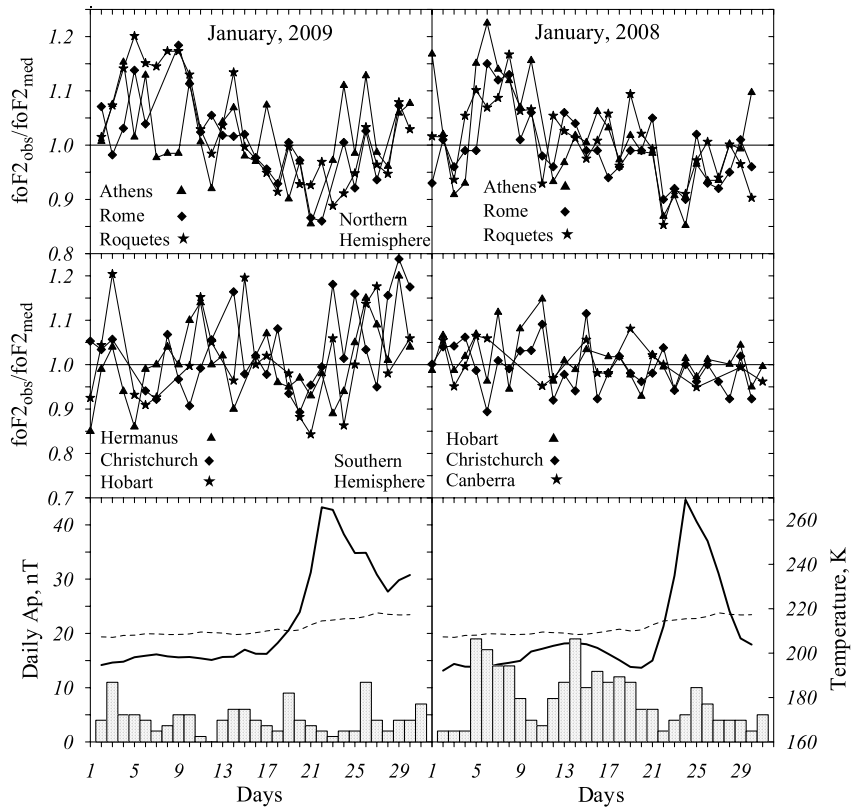

Figure 1. Noontime f_oF_2/f_oF_{2med} ratio for stations located in the Northern (top panel) and Southern (middle panel) Hemispheres during the major SSW event in January 2009 (left column) and the minor event in January 2008 (right column). Bottom panels give daily Ap indices and stratospheric temperature at 90°N, 10 hPa (~32 km), dashed lines—40-year mean values of stratospheric temperature.

3. Results

First let us consider ionospheric (delfoF_2 = foF_{2obs}/foF_{2med}) effects observed simultaneously at middle latitudes in both Hemispheres during a major (January 2009) and a minor (January 2008) Arctic SSW events. Both events took place under a very deep solar minimum and manifest clear SSW impact on the thermosphere not contaminated by solar and geomagnetic activity effects.

On the background of day-to-day foF_{2obs}/foF_{2med} variations in January 2009 (Figure 1) a well-pronounced synchronous foF_2 depression is seen at three European stations and at the stations located in the Southern Hemisphere during some days before and including the SSW maximum on 23 January 2009. The reversal of zonal wind took place on 23/24 January 2009 (MERRA2).

The SSW event in January 2008 manifested a large stratospheric temperature increase (Figure 1, right bottom panel) similar to the major SSW in January 2009 but without a reversal of stratospheric zonal wind therefore formally it is considered as a minor SSW. During this SSW event European stations also manifested a well-pronounced synchronous foF_2 depression during 3 days around the SSW maximum (23–24 January 2008) but no effects are seen at the Southern Hemisphere stations (Figure 1 right column).

The method by Perrone and Mikhailov (2018) was applied at the stations located in the Northern and Southern Hemispheres to retrieve thermospheric parameters during SSW events in question. The results for Rome and Hermanus in January 2009 and for Rome and Hobart in January 2008 are given in Figure 2.

Solar EUV and geomagnetic activity are two external factors controlling the state of thermosphere. Figure 2 shows that solar EUV flux variations were small (~3%) during the analyzed periods and they hardly can be responsible for the revealed variations of thermospheric parameters. Although, ρ, $[O]_{300}$, and T_{ex} seem to follow EUV variations the corresponding correlation coefficients are small and statistically insignificant.

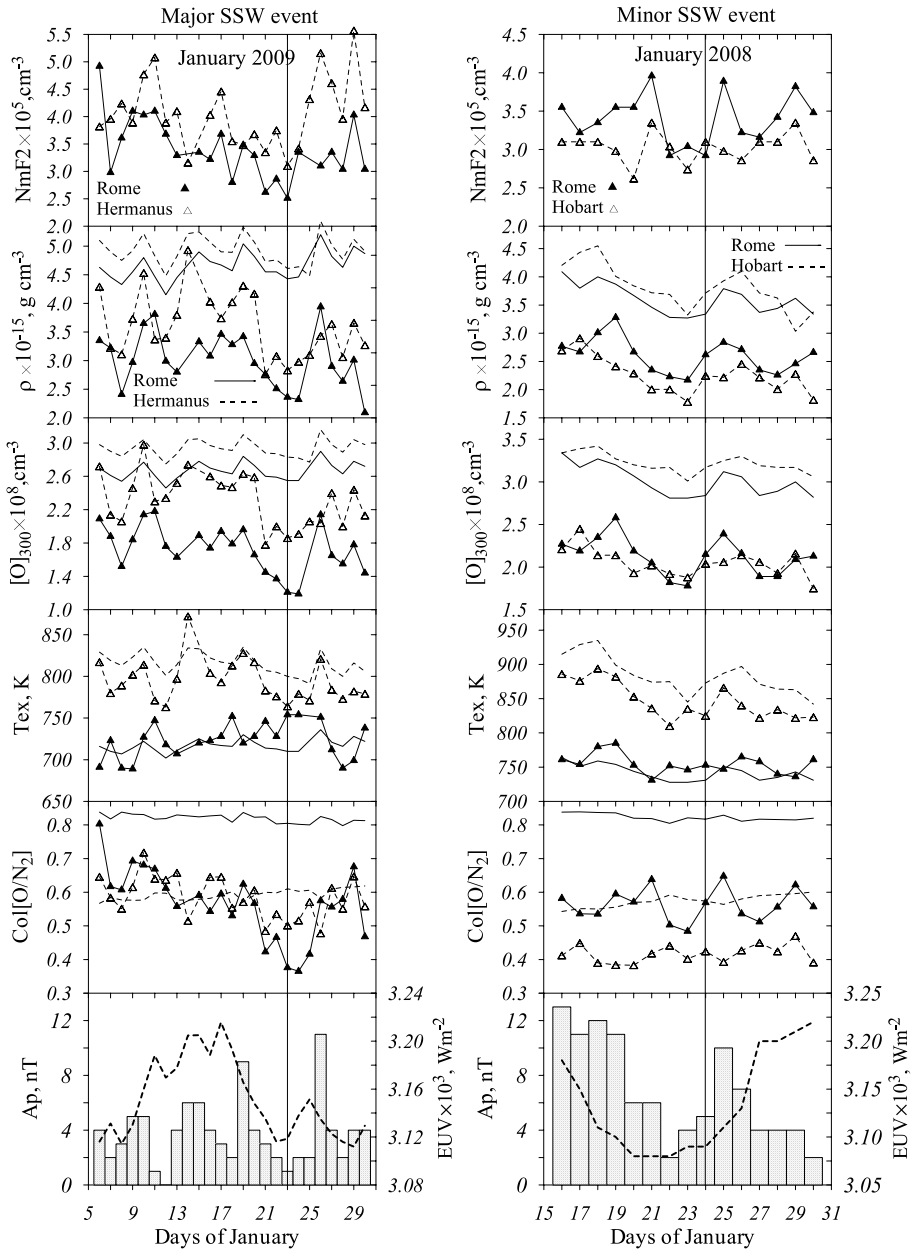

Figure 2. Observed noontime $NmF_2 = 1.24 \times 10^4 (foF_2)^2$, CHAMP/STAR neutral gas densities reduced to 12 LT and station locations along with retrieved atomic oxygen at 300 km, T_{ex}, and column O/N_2 ratio. Model MSISE00 (solid and dashed lines without triangles) variations are given for a comparison. Observed total EUV (100–1200) Å solar flux (Woods et al., 2018) along with Ap indices, are given in the bottom panel. Vertical solid lines indicate the dates of stratospheric temperature peak.

More pronounced effects are related to geomagnetic activity and the reaction depends on season—winter in the Northern and summer in the Southern Hemispheres. The seasonal effect is clearly seen in T_{ex} reaction to magnetic activity especially in January 2009 (Figure 2, left panel). Although magnetic activity was low (Ap ≤ 12 nT) for the periods in question even such individual splashes of Ap index produce visible thermospheric effects under solar minimum as this was shown by Mikhailov et al. (2021). Day-to-day T_{ex}/Ap reaction is clearly seen in summer. This seasonal difference is explained in the framework of well-known thermosphere-ionosphere storm mechanism (Fuller-Rowell et al., 1994; Prölss, 1995; Rishbeth et al., 1987; Rishbeth & Müller-Wodarg, 1999).

Let us consider retrieved thermospheric parameters for 23 January 2009 and 22 January 2008 to manifest the SSW effects. These days were magnetically very quiet with daily Ap ≤ 2 nT. Bearing in mind the obvious dependence

Table 2
Retrieved ρ, [O], [N_2] at 300 km Along With T_{ex} and Column O/N_2 Ratio Are Given for the Selected (23 January 2009 the First Line) and Reference (11 January 2009 the Second Line) Days at Rome and Hermanus

Station	$\rho_{300} \times 10^{-15}$ g cm^{-3}	T_{ex} (K)	$[O]_{300} \times 10^{8}$ cm^{-3}	$[N_2]_{300} \times 10^{7}$ cm^{-3}	Col (O/N_2)
Rome	4.32	754	1.21	2.29	0.38
	6.88	747	2.18	2.28	0.68
	59%	<1%	80%	<1%	79%
Hermanus	6.67	764	1.86	3.60	0.50
	7.85	771	2.31	3.62	0.64
	18%	<1%	24%	<1%	28%

Note. The ratio for reference/selected days in % is given in the third line.

of thermospheric parameters on magnetic activity the reference days selected to visualize the SSW effects should be also very quiet. 11 January 2009 with Ap = 1 nT and 30 January 2008 with Ap = 2 nT were selected as the reference days. The selection of reference period in January 2008 after the SSW peak may raise questions. However, the inferred variations of atomic oxygen and the column O/N_2 ratio indicate (Figure 2, left column) that the duration of atomic oxygen decrease related to SSW is only 3–5 days in the vicinity of the SSW peak. This estimate coincides with the results by Shepherd and Shepherd (2011) on thermospheric O(^{1}S) volume emission rates observed by the WIND Imaging Interferometer on UARS. They observed a depletion above 140 km in the daytime O(^{1}S) volume emission rates, which commenced around the onset of the SSW and lasted over a period of 3–4 days. Therefore, our selection of 30 January 2008 as a reference day is justified. Although the observations by Shepherd and Shepherd (2011) were made at 50°–70°N that is, at slightly larger latitudes than our stations are located (Table 1) our previous analysis (Mikhailov et al., 2021) has shown that Moscow, Juliusruh, and Chilton stations with latitudes >50°N demonstrated a decrease in foF_2 around the SSW peak similar to foF_2 variations at lower latitude Rome, Athens, Roquetes stations. Further, heights considered by Shepherd and Shepherd (2011) are above the turbopause level (~120 km). All neutral species above this level are distributed in accordance with the barometric law at least under magnetically quiet conditions considered in our paper. Therefore, relative variations of [O] (and we consider relative variations in the vicinity of the SSW peak) will be practically same in the whole thermosphere above the turbopause level.

The retrieved thermospheric parameters for the days close to the SSW temperature maxima in January 2009 and 2008 along with same parameters for the reference days are given in Tables 2 and 4.

Table 2 and Figure 2 manifest some interesting results in the Northern Hemisphere.

1. The absence of any essential T_{ex} variations related to SSW contrary earlier obtained results (e.g., Goncharenko & Zhang, 2008; Liu et al., 2011), T_{ex} being close to MSISE00 model values.
2. The absence of any essential [N_2] variations in accordance with the absence of T_{ex} variations. This is an expected result as [N_2] is a chemically inactive species whose distribution is controlled by the barometric law. This result also tells us that processes during SSW do not affect the N_2 abundance in the upper atmosphere.
3. Atomic oxygen demonstrates a strong depletion (~80%) in the vicinity of the SSW maximum compared to the reference day. Although atomic oxygen is the main contributor to neutral gas density at the analyzed heights the latter includes N_2 which is not affected by SSW, therefore quantitatively the decrease in $[O]_{300}$ is larger than in ρ_{300}.
4. Column O/N_2 ratio calculated above the N_2 column density of 10^{17} cm^{-2} (Strickland et al., 1995) manifests solely variations of atomic oxygen during SSW events and this was stressed earlier by Mikhailov et al. (2021).

The Southern Hemisphere (Hermanus) demonstrates similar variations of thermospheric parameters but with much less magnitude than the Northern one: 18% compared to 59% in ρ_{300}, 24% compared to 80% in $[O]_{300}$, 28% compared to 79% in column O/N_2 ratio but similar to Rome—practically no changes take place in T_{ex} and N_2.

Figure 2 manifests that observed neutral gas density and retrieved atomic oxygen qualitatively follow MSISE00 model variations, the latter are driven by solar ($F_{10.7}$) and geomagnetic (Ap) indices. However, quantitatively these variations are different. Figure 3 gives relative variations of ρ, $[O]_{300}$, and T_{ex} calculated with respect to 23

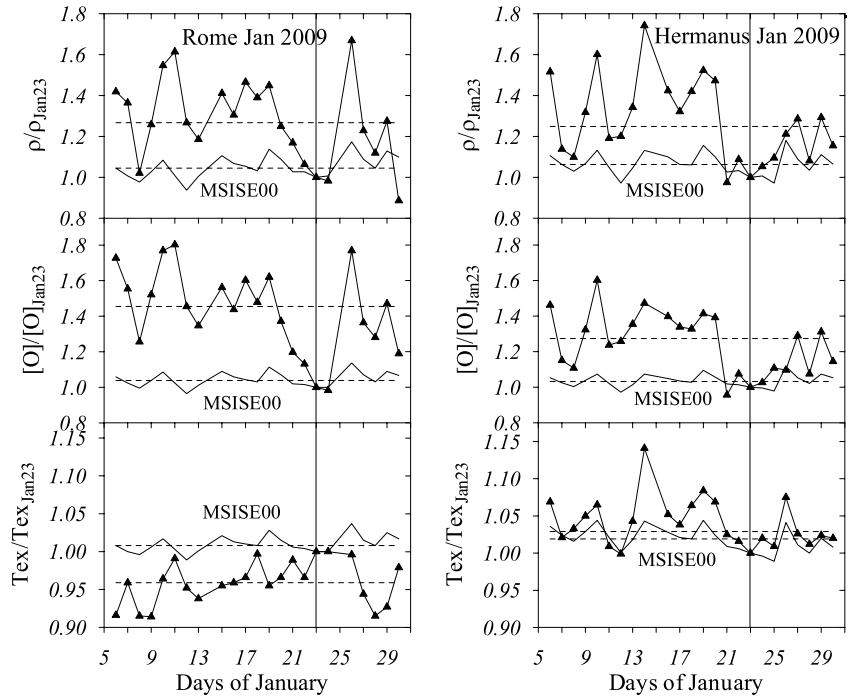

Figure 3. Observed neutral gas density ρ, atomic oxygen $[O]_{300}$, and exospheric temperature T_{ex} variations relative to 23 January 2009 values are given for Rome and Hermanus. Solid lines—MSISE00 model variations. Dashed lines—medians calculated over all points. Vertical solid lines indicate the date of Sudden Stratospheric Warming (SSW) peak.

January (the date of SSW peak) values to demonstrate this difference from MSISE00. Median values (dashed lines) calculated over all available points are given for better obviousness.

MSISE00 is seen to manifest much smaller magnitude of variations compared to observed (ρ) and retrieved ([O] and T_{ex}) parameter variations. Table 3 is given to quantify the difference between medians at Rome and Hermanus.

Table 3 indicates that median relative observed ρ variations are larger on average than MSISE00 predicts by 22% at Rome and by 18% at Hermanus. The difference is larger for atomic oxygen—39% and 23%, correspondingly while practically no difference is seen for T_{ex}. This means that the main SSW effect is related to a decrease of the atomic oxygen abundance in the thermosphere as [O] is the main contributor to neutral gas density at heights of CHAMP/STAR observations (~323 km at Rome and ~332 km at Hermanus). The other important result is that the thermospheric SSW effect is seen in both hemispheres but it is stronger in the Northern hemisphere than in the Southern one during the major SSW in January 2009.

It should be stressed that the January 2009 event presents an ideal case for SSW analyses. It occurred under the deepest solar minimum over the whole history of ionospheric observations. Practically invariable solar EUV and extremely low level of geomagnetic activity allows us to attribute the retrieved variations of thermospheric parameters solely to the impact from below. One may consider this SSW event as a standard while other SSW events (see later) are contaminated to more or less extent by solar EUV and geomagnetic activity effects. For instance, the minor SSW event in January 2008 (Figure 1, right column) also took place under the same deep solar minimum but geomagnetic activity was slightly elevated during that period and the analyzed day of 22 January 2008 (although with Ap = 2 nT) was surrounded by disturbed days. Splashes of magnetic activity with Ap = 7–10 nT may produce visible effects under solar minimum (Mikhailov et al., 2021). Table 4 gives the retrieved thermospheric parameters for the minor SSW event in January 2008.

The minor SSW in January 2008 demonstrated a well-pronounced and synchronous foF_2 decrease at three European stations but not in the Southern Hemisphere (Figure 1, right column). Table 4 explains this effect. Similar

Table 3
Median Values of Relative Variations for ρ, $[O]_{300}$, and T_{ex} Taken From Figure 3 to Quantify the Difference Between Observed (Retrieved) and MSISE00 Model Variations

	Rome			Hermanus		
Parameter	ρ	$[O]_{300}$	T_{ex}	ρ	$[O]_{300}$	T_{ex}
Obs (Ret)	1.27	1.45	0.96	1.25	1.27	1.03
MSISE00	1.04	1.04	1.01	1.06	1.03	1.02

Table 4
Retrieved ρ, [O], [N_2] at 300 km Along With T_{ex} and Column O/N_2 Ratio Are Given for the Selected (22 January 2008 the First Line) and Reference (30 January 2008 the Second Line) Days at Rome and Hobart

Station	$\rho_{300} \times 10^{-15}$ g cm^{-3}	T_{ex} (K)	$[O]_{300} \times 10^{8}$ cm^{-3}	$[N_2]_{300} \times 10^{7}$ cm^{-3}	Col (O/N_2)
Rome	6.17	752	1.82	2.80	0.50
	7.18	761	2.13	3.17	0.56
	16%	1%	17%	13%	12%
Hobart	7.54	810	1.92	5.09	0.44
	7.18	823	1.75	5.28	0.39
	−5%	<2%	−9%	<4%	−11%

Note. The ratio for reference/selected days in % is given in the third line.

the January 2009 SSW case the depression in ρ and $[O]_{300}$ takes place for 22 January (the day before the SSW peak) in a comparison to the reference day, however the magnitude of this depression is much less than for the major SSW in January 2009. By analogy with the major SSW in January 2009 no essential change is seen in T_{ex}. The Southern Hemisphere (Hobart) contrary the January 2009 case manifests small and irregular variations of the thermospheric parameters and this explains the observed irregular foF_2 variations in the vicinity of the SSW maximum date (Figure 1, right column). Therefore, visible SSW effects in the opposite Hemisphere may be expected only for major SSW events.

Two other major SSW events were analyzed to check this conclusion. A major SSW event in January 2013 (Figure 4) with a moderate stratospheric temperature increase ~247 K and a reversal of zonal stratospheric wind on 5 January 2013 manifested a pronounced synchronous foF_2 decrease (~10%) at the European stations during

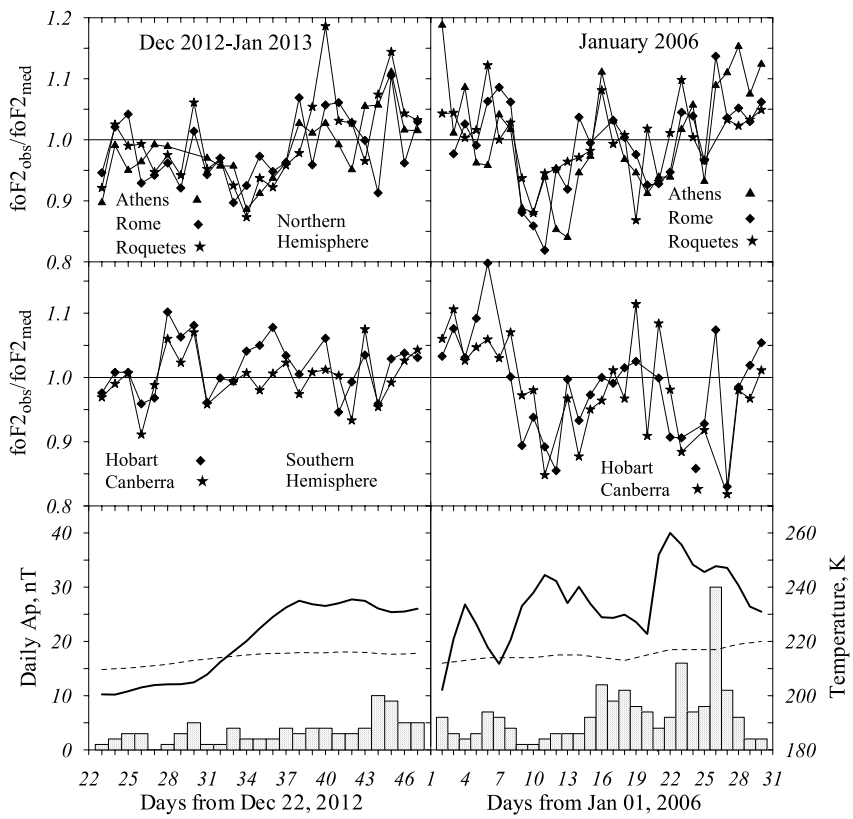

Figure 4. Same as Figure 1 but for major Sudden Stratospheric Warming (SSW) events in January 2013 (left column) and in January 2006 (right column).

some days around January 03, that is, slightly before the SSW temperature maximum. A similar forestalling took place during the January 2009 SSW event. The observed foF_2 depression was not related to geomagnetic activity which was at a very low level (Figure 4, bottom panel). Although that was a major SSW no depression in foF_2 was seen in the Southern Hemisphere at the stations located in the Australian sector (Figure 4, left middle panel).

An interesting three-humped stratospheric temperature major SSW event took place in January 2006 (Figure 4, right panel). The second and third temperature peaks were large enough (244 K on 11 January and 260 K on 22 January) to expect foF_2 deviations comparable to those we had in January 2009. The reversal of zonal wind occurred on 20 January, that is, before the main temperature peak. The main foF_2 effects were associated with the second stratospheric temperature peak. A well-pronounced synchronous foF_2 depression (~15%, around 30% in NmF_2) took place in both Hemispheres around 11 January 2006. It should be stressed that the observed foF_2 decrease also was not related to geomagnetic activity which was very low around this date. It is interesting to note that the magnitudes of foF_2 decrease are comparable in both Hemispheres contrary earlier considered cases. During following on days geomagnetic activity was elevating (Figure 4, right bottom panel) and possible effects of the main stratospheric temperature peak on 22 January were overlapped by increased magnetic activity effects which especially are clearly seen on 26 January when Ap reached 30 nT. In accordance with the F_2-layer storm mechanism midlatitude positive foF_2 deviations took place in the winter Northern Hemisphere and negative ones in the summer Southern Hemisphere after 20 January.

The retrieved and MSISE00 model variations of thermospheric parameters are given in Figure 5.

Unlike two previous SSWs which took place under deep solar minimum (2008–2009) these two major SSW events occurred under elevated solar activity (Figure 5, bottom panels). Solar EUV exhibited a 26% increase during the January 2013 event and the magnitude of EUV variations was within 12% in January 2006. Geomagnetic activity increased from very low in the beginning of both periods toward an elevated one with Ap = 10 nT in January 2013 and moderate one with Ap = 30 nT in January 2006. The continuous increase in EUV and Ap in January 2013 is directly reflected in T_{ex} and $[O]_{300}$ variations for both retrieved and MSISE00 model variations (Figure 5, left middle panels). Similar to SSWs in 2009 and 2008 retrieved T_{ex} does not manifest any reaction to SSW being close to MSISE00 model variations in both Hemispheres. Despite the increase in EUV observed ρ, retrieved $[O]_{300}$ and column O/N_2 ratio demonstrate a pronounced depression at Rome (Northern Hemisphere) with the minimum around January (the peak of SSW). In accordance with foF_2 variations (Figure 4) no pronounced effects next to January 05 are seen in ρ and retrieved $[O]_{300}$ variations at Hobart (Southern Hemisphere). The observed and retrieved variations of thermospheric parameters after the SSW maximum mainly reflect variations of geomagnetic activity bearing in mind different seasons in two Hemispheres. The main conclusion—both observed foF_2 and ρ as well as retrieved $[O]_{300}$ and column O/N_2 ratio do not exhibit any pronounced SSW effects at the stations located in the Southern Hemisphere during the major SSW in January 2013.

The situation with the January 2006 SSW event is more complicated. The second peak in stratospheric temperature on 11 January (Figure 4) practically coincides with the minimum in solar EUV (Figure 5, right bottom panel) therefore the origin of a well-pronounced foF_2 depression in two Hemispheres (Figure 4) may present an overlapped effect of SSW and EUV. However, the analysis shows that this coincidence may not be crucial. On one hand, similar to earlier analyzed SSW cases the retrieved T_{ex} variations are close to MSISE00 model ones and do not manifest any visible SSW effects (Figure 5). Both model and retrieved ρ and $[O]_{300}$ qualitatively follow Ap index variations. On the other hand, both MSISE00 and solar EUV (see, for instance, the EUVAC model by Richards et al. (1994)) depend practically on same $F_{10.7}$ indices: $FA_{10.7}$ (81-day average of $F_{10.7}$ centered on a given day) and daily $F_{10.7}$. In the case of MSISE00 $F_{10.7}$ for previous day are used but normally they are close to daily ones. Therefore, one may think that observed EUV variations are properly reflected (via $F_{10.7}$ indices) in MSISE00 and the quantitative difference between model and retrieved ρ and $[O]_{300}$ (Figure 5) should be attributed to the SSW impact on the upper atmosphere. This SSW effect is large enough—at Rome, for instance, the reduction of ρ and $[O]_{300}$ from January 03 to January 13 (same Ap = 3 nT for both dates) is ~40% while MSISE00 gives ~10% only. Even larger difference ~55% in the retrieved ρ and $[O]_{300}$ takes place at Hobart.

An amazing coincidence not met in other analyzed cases of the retrieved ρ and $[O]_{300}$ variations in two Hemispheres (Figure 5, right middle panels) is due to the T_{ex} and [O] interplay. Of course, seasonal (winter/summer) difference in T_{ex} and in the atomic oxygen abundance exists but lower [O] at the thermospheric bottom is compensated by larger T_{ex} in summer, vice versa situation takes place in winter. Column O/N_2 ratio which does not depend on the neutral temperature profile clearly manifests this seasonal difference in the atomic oxygen

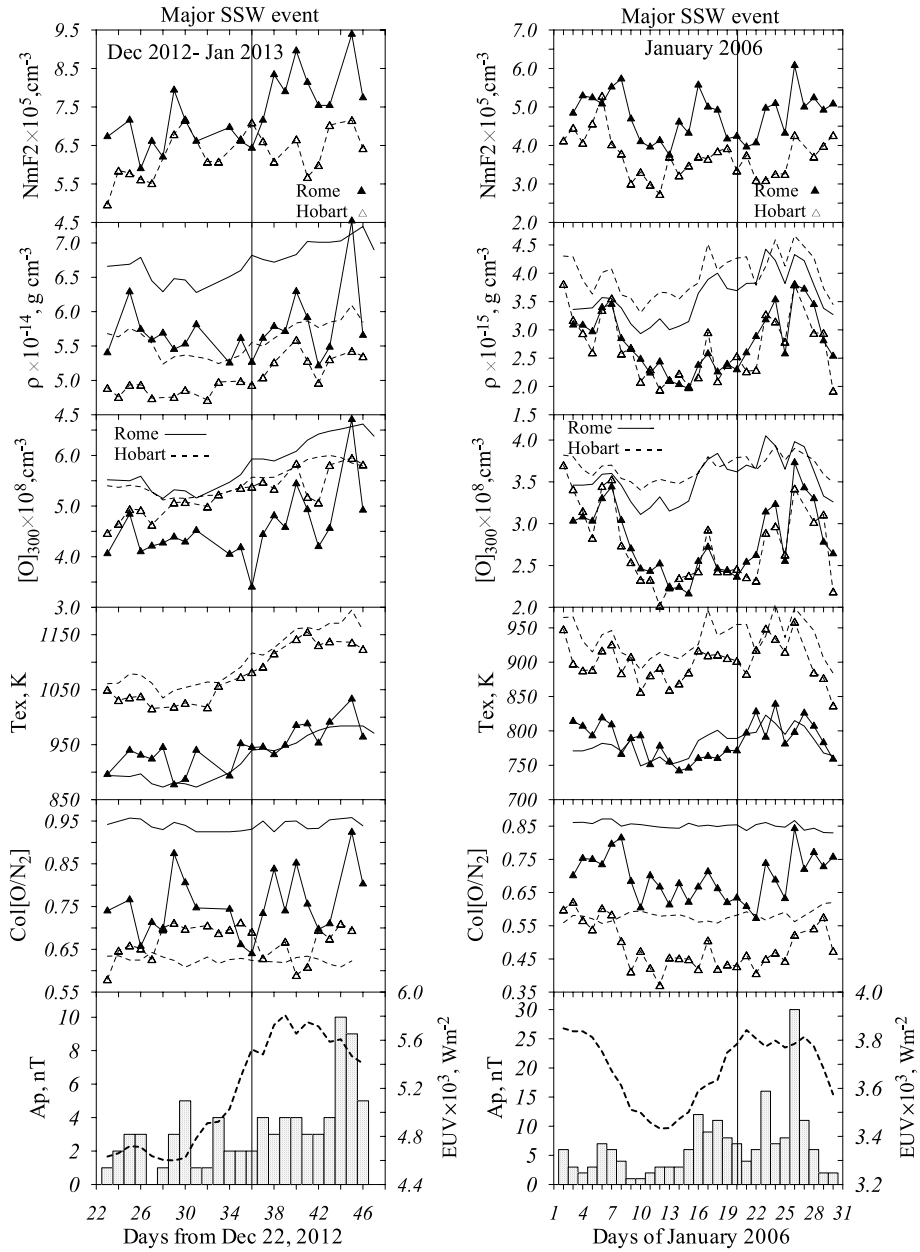

Figure 5. Same as Figure 2 but for the major January 2013 and January 2006 Sudden Stratospheric Warming (SSW) events. GOCE neutral gas density observations were used for the January 2013 event. Vertical lines indicate the stratospheric zonal wind reversal dates.

abundance (Figure 5, bottom). It should be stressed that O/N_2 ratio in fact indicates the column density of atomic oxygen (Mikhailov et al., 2021, their Figure 10).

The undertaken analysis has shown that Arctic SSWs (both major and minor) always result in a pronounced and synchronous foF_2 depression ~(10–15)% at midlatitude European stations starting slightly before the stratospheric temperature peak and lasting for some days. The reaction of midlatitude stations in the Southern Hemisphere to Arctic SWWs may be different—a synchronous (at some stations) foF_2 depression takes place during strong major (January 2009 and January 2006) SSW events but no pronounced foF_2 depression is seen during weak major (January 2013) and minor (January 2008) SWWs. The foF_2 depressions in both Hemispheres are due to a decrease in the atomic oxygen abundance in the upper atmosphere as this was shown earlier by Mikhailov et al. (2021) while T_{ex} does not manifests any visible reaction to SSWs being close to MSISE00 model values.

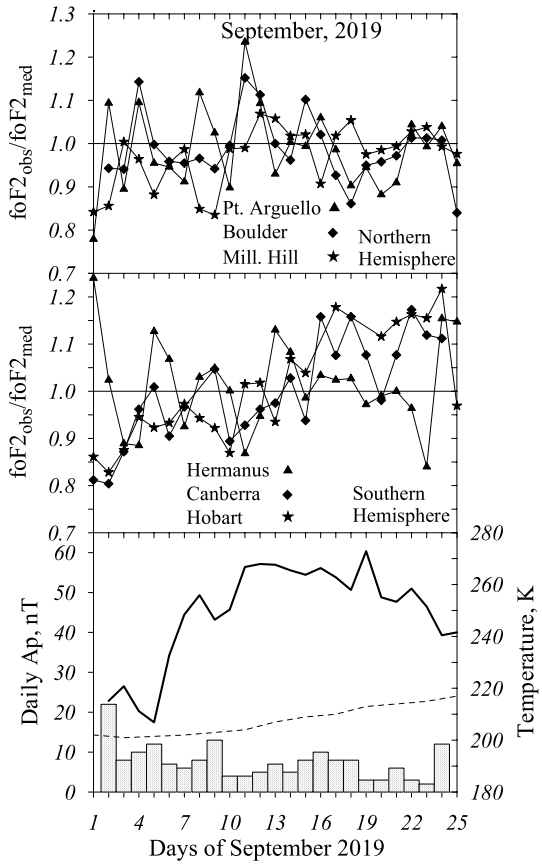

Figure 6. Same as Figure 1 but for the Antarctic Sudden Stratospheric Warming (SSW) in September 2019.

Now let us consider the minor Antarctic SSW event in September 2019. The reaction of Northern Hemisphere to this event in American and European longitudinal sectors was analyzed by Goncharenko, Harvey, Greer, et al. (2021). They have revealed a persistent (at least 30 days) and strong (up to 80–100%) positive anomalies in the daytime TEC in the western region of North America. However, central and eastern parts of North America manifested a very moderate TEC decrease. Therefore, an analysis of the thermosphere reaction to this Antarctic SSW looks very interesting from ionospheric and thermospheric points of view.

Figure 6 gives observed foF_2/foF_{2med} ratio at six midlatitude stations Point Arguello, Millstone Hill, Boulder located in the North America and Hermanus, Canberra, and Hobart located in the Southern Hemisphere. Despite a strong (>60 K) stratospheric temperature increase during the SSW event two groups of stations do not manifest any synchronous reaction contrary the cases we saw earlier with Arctic SSWs. We have just a scatter of foF_2/foF_{2med} within ±20% at these stations. Large foF_2/foF_{2med} scatter may be related to elevated magnetic activity with Ap ≥ 10 nT for some days during the period in question. No visible pronounced difference is seen in foF_2/foF_{2med} between Point Arguello and Millstone Hill which could explain large difference in TEC observed by Goncharenko, Harvey, Greer, et al. (2021). It should be reminded that F_2-layer provides the main contribution to TEC.

Thermospheric parameters were extracted with our method at Point Arguello and Millstone Hill for September 2019. Swarm neutral gas density observations were used in the retrieval process as a fitted parameter. Since no pronounced synchronous foF_2 depressions are seen at the two stations (Figure 6) median values of the retrieved thermospheric parameters calculated over all available points are considered in Table 5. The retrieved hmF_2 and vertical plasma drift W are also given in Table 5.

The analysis of data in Table 5 shows that the difference between Point Arguello and Millstone Hill in observed ρ, retrieved $[O]_{300}$ and T_{ex} is statistically insignificant according to t-criterion. The retrieved column O/N_2 ratio at Point Arguello is slightly larger than at Millstone Hill but MSISE00 also manifests this longitudinal difference. The difference between two stations in retrieved hmF_2 is statistically significant at the 99% confidence level—hmF_2 is slightly larger at Point Arguello due to larger W but the difference in hmF_2 as well as SD are within the height step of 5 km used in the numerical method. Therefore, in fact the difference in hmF_2 between two stations is not essential.

Table 5
Median Values With ±SD Are Given for: Observed Swarm Neutral Gas Densities Reduced to 12 LT and the Location of Stations, Retrieved [O] at 300 km, T_{ex}, and Column O/N_2 Ratio in a Comparison With MSISE00, Calculated hmF_2 and Vertical Plasma Drift W Related to Thermospheric Neutral Winds

Parameter	Point Arguello	Millstone Hill
ρ_{obs} (10^{-16} g cm^{-3})	1.98 ± 0.36	2.15 ± 0.33
$[O]_{300}$ (10^8 cm^{-3})	1.95 ± 0.23	1.88 ± 0.15
T_{ex} (K)	778 ± 21.3	782 ± 23.9
Column $[O/N_2]_{ret}$	0.507 ± 0.079	0.476 ± 0.064
Column $[O/N_2]_{MSISE00}$	0.712 ± 0.036	0.690 ± 0.031
$hmF_{2\,ret}$ (km)	230 ± 3.21	225 ± 4.96
W (m s^{-1})	−9.0 ± 1.98	−10.2 ± 3.07

Note. The total number of analyzed dates is ~20.

Summarizing the results of this consideration it may be stressed that no statistically significant difference in the observed neutral gas density and retrieved thermospheric parameters takes place in September 2019 comparing western (Point Arguello) and eastern (Millstone Hill) regions of North America. Observed foF_2 also did not manifest any visible difference between two stations during this SSW period. Therefore the (80–100%) increase in TEC observed by Goncharenko, Harvey, Greer, et al. (2021) in the western region of North America (in the vicinity of Point Arguello) was not related with changes of thermospheric parameters during the SSW event.

4. Discussion

The undertaken analysis has led us to results which agree only partly with earlier revealed SSW effects in the midlatitude ionospheric F_2-region and in the thermosphere. There is a widely spread opinion that SSWs have a global appearance (Liu et al., 2013; Pedatella et al., 2018; Pedatella & Maute, 2015; Yamazaki et al., 2015 see also Goncharenko, Harvey, Liu, &

Pedatella, 2021). However, our analysis of four SSW events has shown that midlatitude F_2-region of the Southern Hemisphere may not react to Arctic SSWs. Speaking about the reaction we mean a synchronous foF_2 decrease simultaneously observed at some midlatitude ionospheric stations of a given Hemisphere. This effect should be distinguished from day-to-day foF_2 variations (Mikhailov et al., 2021) which do not manifest the synchronism in their occurrence at different stations. The main thermospheric effect of SSWs is a global-scale decrease of the atomic oxygen abundance in the upper atmosphere. This [O] decrease is directly reflected in the NmF_2 depression as $NmF_2 \sim [O]_{300}^{4/3}$ (Mikhailov et al., 1995). Therefore, a synchronous foF_2 depression (not related to magnetic activity) observed at some stations near the SSW maximum should be considered as a direct indication of the SSW impact. The retrieved [O] variations for the SSW periods confirm this conclusion (Figures 2 and 5). We have such synchronous foF_2 depressions in two Hemispheres during the SSW in January 2009 (Figure 1) and in January 2006 (Figure 4). Other two SSW events in January 2008 and January 2013 resulted in synchronous foF_2 depressions only in the Northern Hemisphere. Therefore, not all SSWs have global appearance.

Another interesting aspect of SSW impact on the upper atmosphere is the thermospheric cooling—this is a generally accepted point of view (e.g., Goncharenko, Harvey, Liu, & Pedatella, 2021). Omitting numerous model simulations of SSW events which manifest large disagreement among models in the thermosphere (Pedatella et al., 2014) we will consider some observational results indicating the cooling effect during SSWs. Liu et al. (2011) analyzed CHAMP and GRACE neutral gas density (ρ) observations during the major SSW in January 2009 and their results may be compared to ours. The authors revealed a significant ρ decrease across both hemispheres with the minimum on January 24 (1 day after the SSW peak) in the afternoon (16–18) LT sector. Latitudinal variations of $\Delta\rho$ (their Figure 2) indicate a prolonged and continuous ρ decrease moving toward the date of the SWW maximum. They have chosen 15 January 2009 as a reference day with large observed neutral gas density (Figure 2). If they took a reference day with low Ap index similar to Ap on 23–24 January their plot would be quite different with the maximal ρ decrease during only 2–3 days around the SSW peak on 23 January. A 50 K drop in thermospheric neutral temperature in the equatorial 30°S−30°N region was obtained in the paper and this temperature decrease was confirmed by MSISE00 calculations if model ρ values were fitted to the observed ones. It should be stressed that the magnitude of temperature decrease also depends on the chosen background used for a comparison with the 24 January value. MSISE00 is driven by observed solar ($F_{10.7}$) and magnetic (Ap) indices and it does not take into account the atomic oxygen decrease (which is essential, see Table 2) related to SSW (Figure 2). Atomic oxygen is the main contributor to neutral gas density at CHAMP and GRACE heights.

Further, Liu et al. (2011) have found that the Southern Hemisphere experienced a larger relative density decrease than the Northern one. In fact, this depends on latitude. If CHAMP observations at middle latitudes (±40°) in two Hemispheres are compared, no difference is seen for dates before the SSW peak. On 24 January, the Northern Hemisphere manifested larger $\Delta\rho$ (their Figure 2). So, one may conclude that neutral density decrease was larger in the Hemisphere of SSW occurrence in accordance with our results (Table 2).

Yamazaki et al. (2015) have considered satellite drag data (~5,000 objects) for the January 1967 to December 2013 period and examined 37 SSW events. A superposed epoch analysis revealed a density reduction of 3%–7% at 250–575 km around the time of maximum polar vortex weakening. The temperature perturbation was estimated to be -7.0 ± 2.5 K K at 400 km.

It is not that easy to estimate neutral temperature variations from satellite drag observations keeping in mind that ρ depends both on neutral temperature and composition, atomic oxygen concentration (the main contributor to ρ) being not known in that analysis and the authors stress this. Moreover, they worked with global averaged density observations obtained in two Hemispheres under different (winter/summer) seasons and local times. This inevitably results in different relative neutral composition and so different mean molecular mass M used to infer neutral temperature. Their expression (3) used in the paper was derived with some assumptions and constraints which are not discussed in the paper. An additional complication affecting the results is the asymmetry of SSWs appearance in two Hemispheres - not all Arctic SSWs are seen in the Southern Hemisphere as this was shown in our analysis. All this resulted in a 3–7% global neutral density decreases while any analysis of individual SSWs using local ρ observations gives much larger ρ depressions related to SSWs. For instance, Figure 1 from Yamazaki et al. (2015) gives a global mean ρ decrease ~20% comparing 11 January to 23 January 2009 with close Ap indices while our analysis gives ρ decrease of 59% at Rome and 18% at Hermanus (Table 2).

It should be stressed that the revealed decrease in the atomic oxygen abundance (Table 2) is larger than the expected inaccuracy of the method by Perrone and Mikhailov (2018).

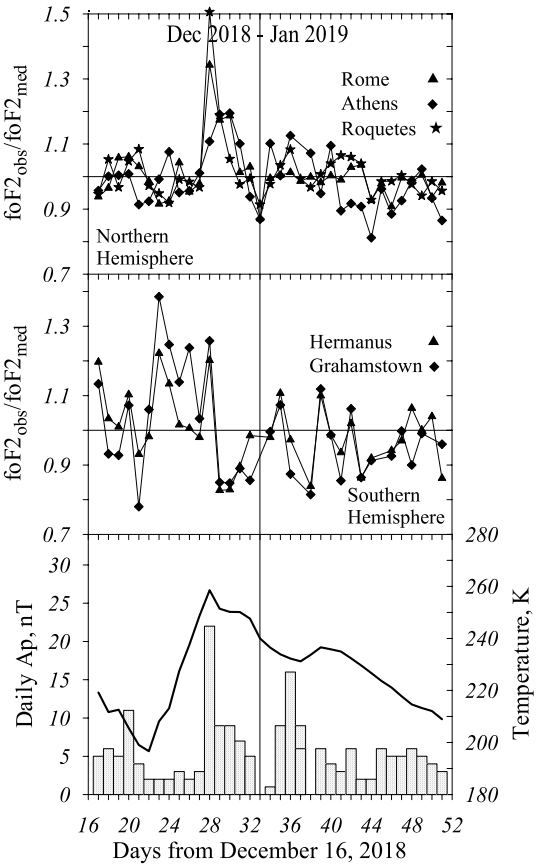

Figure 7. Same as Figure 1 but for December 2018 to January 2019 major Sudden Stratospheric Warming (SSW). Vertical line indicates the date of zonal wind reversal.

On the other hand, Yamazaki et al. (2015) gave a very small (~7 K) depression in T_{ex} which looks as a reasonable one compared to ~50 K obtained by Liu et al. (2011). Our analysis has not also revealed any pronounced T_{ex} depressions related to SWWs (Figures 2 and 5).

Global-Scale Observations of the Limb and Disk (GOLD) instrument on the geostationary SES-14 communications satellite revealed a substantial response of the mean state of the thermosphere to the major Sudden Stratospheric Warming (SSW) event in December 2018 to early January 2019 (Oberheide et al., 2020). According to MERRA2 the stratospheric temperature maximum of 258.5 K was reached on 28 December 2018 and the reversal of zonal wind took place on 2 January 2019. Observed foF_2/foF_{2med} variations at the stations located in two Hemispheres in the same longitudinal sector are given in Figure 7.

A sharp decrease of (10–15)% in the column O/N_2 ratio has started on 23 December 2018 (their Figure 1c) mainly in the Northern Hemisphere and lasted for ~3 days. This column O/N_2 ratio decrease took place under low magnetic activity (Figure 7) and resulted in a nonsynchronous foF_2 depression (~10%) at the European stations and a pronounced up to 30% foF_2 increase in the Southern Hemisphere, the mechanism of this foF_2 increase should be yet explained in future. A strong increase of magnetic activity on December 28 has resulted (in accordance with the F_2-layer storm mechanism) in a large foF_2 increase in the winter Hemisphere and a foF_2 decrease in the summer one (Figure 7).

The second wave of column O/N_2 ratio decrease (~10%) has started on 1 January and was mainly observed in the equatorial and middle latitudes of the Northern Hemisphere (their Figure 1c). Its onset exactly coincided in time with the reversal of zonal wind (MERRA2). Similarly earlier analyzed SSW events this O/N_2 ratio decrease resulted in a synchronous foF_2 depression at three European stations without any visible effects in the Southern Hemisphere. The observed column O/N_2 ratio decrease (~10%) is too small compared to (~80%) retrieved for the strong major SSW in January 2009 (Table 2) but it is close to ~12% O/N_2 ratio decrease retrieved for the minor SSW in January 2008 (Table 4) with a similar foF_2 decrease only in the Northern Hemisphere (Figure 1 right column). Thus, we may conclude that a synchronous at some stations foF_2 depression may be considered as the indicator of the column O/N_2 ratio decrease related to SSWs event. Earlier we saw this effect using retrieved thermospheric parameters, direct observations by Oberheide et al. (2020) gave the same result. The analyzed major SSW event also confirms our earlier formulated result—ionospheric and thermospheric SSW effects are mainly seen in the Hemisphere of the SSW origin.

All analyzed SSW events were Arctic ones and the first attempt to consider the ionospheric and thermospheric effects of an Antarctic SSW was undertaken by Goncharenko, Harvey, Greer, et al. (2021). They have considered a minor Antarctic SSW event in September 2019. The obtained results raise some questions.

1. What in fact the authors have observed speaking about TEC positive anomaly (up to 80–100%) in western part of North America and the absence of any noticeable effects in the central and eastern parts of U.S.? Our analysis has shown no significant difference between two regions both in NmF_2 and in thermospheric parameter variations during September 2019. F2-region is the main contributor to TEC (Lee et al., 2013), therefore under similar NmF_2 in the two regions one should not expect any TEC positive anomaly at Point Arguello during this event. However, one should bear in mind that TEC consists of the ionospheric TEC (ITEC) and plasmaspheric PTEC parts. Global morphological analysis by Lee et al. (2013, their Figure 3), of plasmaspheric PTEC and ionospheric ITEC has shown that normally ITEC is ~12 TECU and PTEC is ~3 TECU, that is, PTEC is ~25% of ITEC for the conditions in question: equinox, solar minimum, low magnetic activity, northern hemisphere, magnetic latitude ~42°, noontime hours. With a doubled TEC (Goncharenko, Harvey, Greer, et al., 2021) under unchanged ITEC, PTEC should be 30 − 12 = 18 TECU. This is larger than normally observed ITEC by 1.5 times. The situation when PTEC is larger than ITEC under the conditions in question is not confirmed by observations (Lee et al., 2013, also Yizengaw et al., 2008);

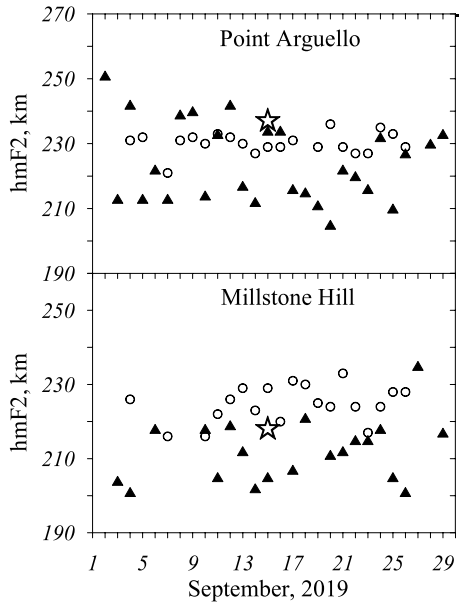

Figure 8. Observed with DPS-4 noontime (triangles) and retrieved (circles) hmF_2 at Point Arguello and Millstone Hill in September 2019. Asterisks—monthly median noontime hmF_2 values (Shubin, 2015).

2. Is it possible to explain the observed TEC anomaly with a 10% increase in column O/N_2 ratio and zonal component *Vny* of thermospheric wind modulated by SSW? On one hand, a 10% increase in column O/N_2 is not sufficient to explain the observed (80–100%) TEC positive anomaly bearing in mind that electron concentration in the F_2-layer is the main contributor to TEC (Lee et al., 2013). On the other hand, the contribution of zonal Vny wind to vertical plasma drift is relatively small compared to meridional *Vnx* one during daytime hours as this follows from empirical models (Drob et al., 2015; Hedin et al., 1991, 1996) and CHAMP observations of thermospheric zonal winds at low and middle latitudes (Zhang et al., 2018). Vertical plasma drift $W = (Vnx\cos D - Vny\sin D)$ sin IcosI where *Vnx*—positive to the South, *Vny*—positive to the East, *D*—magnetic declination positive to the East, *I*—magnetic inclination positive in the Northern hemisphere where the vector of total magnetic field *B* is downward. Magnetic declination *D* is ~10° (eastward) in the area of positive TEC anomaly (western part of U.S., their Figure 2). If thermospheric zonal wind plays a major role as Goncharenko, Harvey, Greer, et al. (2021) suggest then *Vny* should be strong enough to compensate at least the negative effect of *Vnx* in noontime NmF_2. In case when *Vny* (upward plasma drift) compensates the effect of *Vnx* (downward plasma drift) $Vny = Vnx\cos D/\sin D = 5.76 \times Vnx$. Normally noontime midlatitude $Vnx \sim 50$ m/s is poleward under magnetically quiet conditions (Drob et al., 2015; Hedin et al., 1991, 1996). This gives $Vny \sim 290$ m/s. Such daytime zonal winds are not predicted either by empirical wind models or CHAMP observations of thermospheric zonal winds at low and middle latitudes (Zhang et al., 2018). Similar TEC increase in the European sector on 21 September 2019 at 14UT (their Figure 2) in principle cannot be discussed in terms of Vny as $D \sim 0°$ in this area.

An increase of daytime *Vny* should be very large to produce a noticeable NmF_2 increase. But ionosonde observations do not manifest such an increase in the second part of September (Figure 6). Moreover, an increase of *Vny* and a corresponding increase in vertical plasma drift *W* should be seen in hmF_2 variations but DPS-4 observations do not show this. Figure 8 gives observed with DPS-4 noontime hmF_2 in a comparison to our retrieved and monthly median model (Shubin, 2015, this model now is in IRI) values for Point Arguello and Millstone Hill. The retrieved as well as model median hmF_2 on average are somewhat larger than observed ones but this is due to the method of ionogram reduction in DPS-4 (Chen et al., 1994)—the last point on ionogram (without an extrapolation) is taken as hmF_2 (see also Krasheninnikov & Leshchenko, 2021).

Our retrieved hmF_2 and W are close at the two stations (Table 5). Therefore, western and eastern regions of U.S. manifest normal quite time behavior of ionospheric and thermospheric parameters during the September 2019 SSW event and the observed (80–100%) TEC increase was not related to thermospheric parameters (neutral composition, temperature, winds) but may reflect an increase of electron concentration in the high-latitude ionosphere projected to the plasmasphere of middle latitudes.

5. Conclusions

The reaction of midlatitude daytime thermospheric parameters and foF_2 to SSWs has been analyzed in two Hemispheres for the periods of a minor Arctic SSW in January 2008, three major Arctic SSWs in January 2006, 2009, 2013, and a minor Antarctic SSW in September 2019. The obtained results may be formulated as follows:

1. Arctic SSWs (both major and minor) always result in a synchronous simultaneously observed at some stations foF_2 depression ~(10–15)% at midlatitude European stations starting slightly before the SSW peak and lasting for some days. Our analysis of four SSW events has shown that midlatitude F_2-region of the Southern Hemisphere may not react to Arctic SSWs therefore not all SSWs have global appearance. Synchronous foF_2 depressions (not related to geomagnetic activity) in the Southern Hemisphere took place during strong major January 2009 and 2006 SSW events but no pronounced foF_2 effects were seen during a weak major (January

2013) and a minor (January 2008) SWW events. Thus, SSW effects in foF_2 are always seen in the Hemisphere of the SSW occurrence but not necessary in the opposite Hemisphere.

2. The main thermospheric SSW effect is a decrease of the atomic oxygen abundance also seen in the observed neutral gas density and in the retrieved column O/N_2 ratio. A smaller magnitude of foF_2 variations in the Southern Hemisphere compared to the Northern one during the strong January 2009 SSW is also seen in thermospheric parameter variations (Figure 1 and Table 2): 18% compared to 59% in ρ_{300}, 24% compared to 80% in $[O]_{300}$, and 28% compared to 79% in column O/N_2 ratio. Similar foF_2 variations in two Hemispheres during another strong SSW in January 2006 (Figure 4) are reflected in similar variations of thermospheric parameters (Figure 5). In contrast to strong SSWs the minor SSW event in January 2008 resulted in smaller ρ_{300}, $[O]_{300}$, and O/N_2 ratio depressions in the Northern Hemisphere while the Southern Hemisphere only manifested moderate irregular variations (Table 4). A similar pattern of thermospheric parameter variations without pronounced effects in the Southern Hemisphere took place during the major but weak SSW event in January 2013. Therefore, pronounced thermospheric SSW effects in the opposite (Southern) Hemisphere may be expected only for strong major Arctic SSW events.
3. Contrary to generally accepted view retrieved exospheric temperature T_{ex} does not manifest any visible reaction to SSWs both for major and minor SSW events (Figures 2 and 5 and Tables 2 and 4).
4. The duration of foF_2 and atomic oxygen decrease related to SSW is 3–5 days in the vicinity of the SSW peak. This estimate coincides with the results by Shepherd and Shepherd (2011) on thermospheric $O(^1S)$ volume emission rate observations. This result contradicts a widely spread opinion about long duration of SSW effects in the thermosphere.
5. Strong (80–100%) TEC increase observed by Goncharenko, Harvey, Greer, et al. (2021) in the western region of North America during the minor Antarctic SSW in September 2019 was not related with variations of thermospheric neutral composition and winds.

Data Availability Statement

The European Space Agency provides Swarm (https://earth.esa.int/eogateway/catalog/swarm-ionosphere-magnetosphere) the GFZ German Research Center for CHAMP data (ftp://anonymous@isdcftp.gfz-potsdam.de/champ/) and Woods for EUV observations (http://lasp.colorado.edu/lisird/). The Rome ionospheric data are provided by INGV (https://doi.org/10.13127/eswua/hf), as the Lowell DIDBase through GIRO for ionosonde data (http://giro.uml.edu/). NOAA SWPC (https://www.swpc.noaa.gov/), GFZ Potsdam (https://www.gfz-potsdam.de/en/kp-index/), the WDC for Geomagnetism, Kyoto (http://wdc.kugi.kyoto-u.ac.jp/wdc/Sec3.html) for geomagnetic index ap and MERRA-2 for stratospheric temperature (https://disc.gsfc.nasa.gov/datasets?project=MERRA-2).

Acknowledgments
This research was carried within the INGV Pianeta Dinamico Project (CUP D53J19000170001), The Solar wind—Earth's magnetosphere Relationships and their Effects on ioNosphere and upper and lower Atmosphere (SERENA)—2021, funded by MUR (law 145/2018). The authors thanks for the Ionosonde data the GIRO group http://spase.info/SMWG/Observatory/GIRO.
Data from the South African Ionosonde network is made available through the South African National Space Agency (SANSA), who are acknowledged for facilitating and coordinating the continued availability of data. This publication uses data from: the ionospheric observatory in Roquetes, Spain, owned and operated by the Fundació Observatori de l'Ebre; from the Juliusruh Ionosonde which is owned by the Leibniz Institute of Atmospheric Physics Kuehlungsborn. The responsible Operations Manager is Jens Mielich; from the ionospheric observatory in Dourbes, owned and operated by the Royal Meteorological Institute (RMI) of Belgium.

References

Chen, C. F., Reinisch, B. W., Scali, J. L., Huang, X., Gamache, R. R., Buonsanto, M. J., & Ward, B. D. (1994). The accuracy of ionogram-derived N(h) profiles. *Advances in Space Research*, *14*(12), 43–46. https://doi.org/10.1016/0273-1177(94)90236-4

Drob, D. P., Emmert, J. T., Meriwether, J. W., Makela, J. J., Doornbos, E., Conde, M., et al. (2015). An update to the Horizontal Wind Model (HWM): The quiet time thermosphere. *Earth and Space Science*, *2*(7), 301–319. https://doi.org/10.1002/2014EA000089

Fuller-Rowell, T. J., Codrescu, M. V., Moffett, R. J., & Quegan, S. (1994). Response of the thermosphere and ionosphere to geomagnetic storm. *Journal of Geophysical Research*, *99*, 3893–3914.

Goncharenko, L., Harvey, V. L., Liu, H., & Pedatella, N. (2021). Sudden stratospheric warming impacts on the ionosphere-thermosphere system - A review of recent progress. In C. Huang & G. Lu (Eds.), *Advances in ionospheric research: Current understanding and challenges*, *Space physics and aeronomy* (Vol. 3). Wiley.

Goncharenko, L. P., Harvey, V. L., Greer, K. R., Zhang, S.-R., Coster, A. J., & Paxton, L. J. (2021). Impact of September 2019 Antarctic sudden stratospheric warming on mid-latitude ionosphere and thermosphere over North America and Europe. *Geophysical Research Letters*, *48*, e2021GL094517. https://doi.org/10.1029/2021GL094517

Goncharenko, L. P., & Zhang, S.-R. (2008). Ionospheric signatures of sudden stratospheric warming: Ion temperature at middle latitude. *Geophysical Research Letters*, *35*, L21103. https://doi.org/10.1029/2008GL035684

Hedin, A. E., Biondi, M. A., Burnside, R. G., Hernandez, G., Johnson, R. M., Killeen, T. L., et al. (1991). Revised global model of thermosphere winds using satellite and ground-based observations. *Journal of Geophysical Research*, *96*(A5), 7657–7688. https://doi.org/10.1029/91JA00251

Hedin, A. E., Fleming, E. L., Manson, A. H., Schmidlin, F. J., Avery, S. K., Clark, R. R., et al. (1996). Empirical wind model for the upper, middle and lower atmosphere. *Journal of Atmospheric and Solar-Terrestrial Physics*, *58*(13), 1421–1447. https://doi.org/10.1016/0021-9169(95)00122-0

Krasheninnikov, I. V., & Leshchenko, L. N. (2021). Errors in estimating of the *F*2-layer peak parameters in automatic systems for processing the ionograms in the vertical radio sounding of the ionosphere under low solar activity conditions. *Geomagnetism and Aeronomy*, *61*(5), 599–609. https://doi.org/10.1134/s0016793221050078

Lee, H.-B., Jee, G., Kim, Y. H., & Shim, J. S. (2013). Characteristics of global plasmaspheric TEC in comparison with the ionosphere simultaneously observed by Jason-1 satellite. *Journal of Geophysical Research: Space Physics*, *118*, 935–946. https://doi.org/10.1002/jgra.50130

Liu, H., Doornbos, E., Yamamoto, M., & Tulasi Ram, S. (2011). Strong thermospheric cooling during the 2009 major stratosphere warming. *Geophysical Research Letters*, *38*, L12102. https://doi.org/10.1029/2011GL047898

Liu, H., Jin, H., Miyoshi, Y., Fujiwara, H., & Shinagawa, H. (2013). Upper atmosphere response to stratosphere sudden warming: Local time and height dependence simulated by GAIA model. *Geophysical Research Letters*, *40*, 635–640. https://doi.org/10.1002/grl.50146

March, G., vanden Ijssel, J., Siemes, C., Visser, P., Doornbos, E., & Pilinski, M. (2021). Gas-surface interactions modelling influence on satellite aerodynamics and thermosphere density. *Journal of Space Weather and Space Climate*, *11*, 54. https://doi.org/10.1051/swsc/2021035

Mikhailov, A. V., Perrone, L., & Nusinov, A. A. (2021). Mid-latitude daytime F2-layer disturbance mechanism under extremely low solar and geomagnetic activity in 2008–2009. *Remote Sensing*, *13*(8), 1514. https://doi.org/10.3390/rs13081514

Mikhailov, A. V., Skoblin, M. G., & Förster, M. (1995). Day-time F2-layer positive storm effect at middle and lower latitudes. *Annales Geophysicae*, *13*(5), 532–540. https://doi.org/10.1007/s00585-995-0532-y

Oberheide, J., Pedatella, N. M., Gan, Q., Kumari, K., Burns, A. G., & Eastes, R. (2020). Thermospheric composition O/N_2 response to an altered meridional mean circulation during Sudden Stratospheric Warmings observed by GOLD. *Geophysical Research Letters*, *47*, e2019GL086313. https://doi.org/10.1029/2019GL086313

Pedatella, N. M., Chau, J. L., Schmidt, H., Goncharenko, L. P., Stolle, C., Hocke, K., et al. (2018). Sudden stratospheric warming impacts on the whole atmosphere. *Eos*, *99*. https://doi.org/10.1020/2017ES005448

Pedatella, N. M., Fuller-Rowell, T., Wang, H., Jin, H., Miyoshi, Y., Fujiwara, H., et al. (2014). The neutral dynamics during the 2009 sudden stratosphere warming simulated by different whole atmosphere models. *Journal of Geophysical Research: Space Physics*, *119*, 1306–1324. https://doi.org/10.1002/2013JA019421

Pedatella, N. M., & Maute, A. (2015). Impact of the semidiurnal lunar tide on the midlatitude thermospheric wind and ionosphere during sudden stratosphere warmings. *Journal of Geophysical Research: Space Physics*, *120*, 10740–10753. https://doi.org/10.1002/2015JA021986

Perrone, L., & Mikhailov, A. V. (2018). A new method to retrieve thermospheric parameters from daytime bottom-Side Ne(h) observations. *Journal of Geophysical Research: Space Physics*, *123*, 10200–10212. https://doi.org/10.1029/2018JA025762

Picone, J. M., Hedin, A. E., Drob, D. P., & Aikin, A. C. (2002). NRLMSISE-00 empirical model of the atmosphere: Statistical comparison and scientific issues. *Journal of Geophysical Research*, *107*(A12), 1468. https://doi.org/10.1029/2002JA009430

Prölss, G. W. (1995). Ionospheric F-region storms. In H. Volland (Ed.), *Handbook of atmospheric electrodynamics* (Vol. 2, pp. 195–248). CRC Press/.

Reinisch, B. W., & Galkin, I. A. (2011). Global ionospheric radio observatory (GIRO). *Earth Planets and Space*, *63*(4), 377–381. https://doi.org/10.5047/eps.2011.03.001

Reinisch, B. W., Galkin, I. A., Khmyrov, G., Kozlov, A., & Kitrosser, D. F. (2004). Automated collection and dissemination of ionospheric data from the digisonde network. *Advances in Radio Science*, *2*, 241–247. https://doi.org/10.5194/ars-2-241-2004

Richards, P. G., Fennelly, J. A., & Torr, D. G. (1994). Euvac: A solar EUV flux model for aeronomic calculations. *Journal of Geophysical Research*, *99*(A5), 8981–8992. https://doi.org/10.1029/94JA00518

Rishbeth, H., Fuller-Rowell, T. J., & Rodger, A. S. (1987). F-layer storms and thermospheric composition. *Physica Scripta*, *36*(2), 327–336. https://doi.org/10.1088/0031-8949/36/2/024

Rishbeth, H., & Müller-Wodarg, I. C. F. (1999). Vertical circulation and thermospheric composition: A modelling study. *Annales Geophysicae*, *17*(6), 794–805. https://doi.org/10.1007/s00585-999-0794-x

Shepherd, M. G., & Shepherd, G. G. (2011). Stratospheric warming effects on thermospheric $O(^1S)$ dayglow dynamics. *Journal of Geophysical Research*, *116*, A11327. https://doi.org/10.1029/2011JA016762

Shubin, V. N. (2015). Global median model of the F2-layer peak height based on ionospheric radio-occultation and ground-based Digisonde observations. *Advances in Space Research*, *56*(5), 916–928. https://doi.org/10.1016/j.asr.2015.05.029

Shubin, V. N., & Deminov, M. G. (2019). Global dynamic model of critical frequency of the ionospheric F2 layer. *Geomagnetism and Aeronomy*, *59*(4), 429–440. https://doi.org/10.1134/s0016793219040157

Siemes, C., de Teixeira da Encarnação, J., Doornbos, E. N., vanden Ijssel, J., Kraus, J., Pereštý, R., et al. (2016). Swarm accelerometer data processing from raw accelerations to thermospheric neutral densities. *Earth Planets and Space*, *68*(1), 92. https://doi.org/10.1186/s40623-016-0474-5

Strickland, D. J., Evans, J. S., & Paxton, L. J. (1995). Satellite remote sensing of thermospheric O/N_2 and solar EUV 1. *Theory. Journal of Geophysical Research*, *100*(A7), 12217–12226. https://doi.org/10.1029/95JA00574

Upper atmosphere physics, radiopropagation Working Group, Marcocci, C., Pezzopane, M., Pica, E., Romano, V., et al. (2020). Electronic Space Weather upper atmosphere database (eSWua)—HF data, version 1.0 (1.0) [Dataset]. Istituto Nazionale di Geofisica e Vulcanologia (INGV). https://doi.org/10.13127/ESWUA/HF

vanden Ijssel, J., Doornbos, E., Iorfida, E., March, G., Siemes, C., & Montenbruck, O. (2020). Thermosphere densities derived from Swarm GPS observations. *Advances in Space Research*, *65*(7), 1758–1771. https://doi.org/10.1016/j.asr.2020.01.004

Woods, T. N., Eparvier, F. G., Harder, J., & Snow, M. (2018). Decoupling solar variability and instrument trends using the multiple same-irradiance-level (MuSIL) analysis technique. *Solar Physics*, *293*(5), 76. https://doi.org/10.1007/s11207-018-1294-5

Yamazaki, Y., Kosch, M. J., & Emmert, J. T. (2015). Evidence for stratospheric sudden warming effects on the upper thermosphere derived from satellite orbital decay data during 1967–2013. *Geophysical Research Letters*, *42*, 6180–6188. https://doi.org/10.1002/2015GL065395

Yizengaw, E., Moldwin, M. B., Galvan, D., Iijima, B. A., Komjathy, A., & Mannucci, A. J. (2008). Global plasmaspheric TEC and its relative contribution to GPS TEC. *Journal of Atmospheric and Solar-Terrestrial Physics*, *70*(11–12), 1541–1548. https://doi.org/10.1016/j.jastp.2008.04.022

Zhang, K., Wang, W., Wang, H., Dang, T., Liu, J., & Wu, Q. (2018). The longitudinal variations of upper thermospheric zonal winds observed by the CHAMP satellite at low and midlatitudes. *Journal of Geophysical Research: Space Physics*, *123*, 9652–9668. https://doi.org/10.1029/2018JA025463